Vesicles prepared with the complex salts dioctadecyldimethylammonium polyacrylates

Fernanda Rosa Alves, Watson Loh *

Institute of Chemistry, Universidade Estadual de Campinas (UNICAMP), Caixa Postal 6154, 13083-970 Campinas, SP, Brazil

A B S T R A C T

The effect of a polymeric counterion on the thermotropic behavior of sonicated vesicles formed by complex salts in aqueous solution and with decanol ($C_{10}OH$) and tetradecanol ($C_{14}OH$) was investigated. The complex salts were prepared with dioctadecyldimethylammonium bromide (DODAB) and polyacrylic acids (PAA, containing 30 or 6000 repeating units), being referred to as $DODAPA_{30}$ and $DODAPA_{6000}$. Vesicles containing polymeric counterions presented higher contents of multilamellar vesicles that were dependent on the complex salt concentration and on the counterion chain length. For comparison, studies were performed with DODAAc, with the counterion acetate, resulting in the formation of mostly unilamellar vesicles, as expected due greater dissociation, leading to greater electrical repulsion between bilayers. Mixtures of these complex salts and DODAX (where X = acetate or bromide) were also investigated with respect to their vesicles thermotropic behavior and size. This study opens the possibility of applying the methodology of direct complex salt preparation (as opposed to mixing the surfactant and polymeric components) to produce vesicles with controlled composition and properties.

© 2011 Elsevier Inc. Open access under the Elsevier OA license.

1. Introduction

Owing to their structural similarity to cell membranes, vesicles have attracted considerable interest as membrane models and as drug delivery vehicles [1–4]. For these applications, properties such as vesicle stability, size, polydispersity, degree of counterion dissociation and thermotropic behavior, represented by the melting temperature, T_m, should be well controlled. Cationic vesicles have been utilized in the condensation of DNA molecules and formation of lipoplexes that are of great importance for in vitro DNA transfection into cells [5–11]. However, the mechanism of interaction between cationic surfactants and polymers, when DNA is substituted for a polyanion, such as polyacrylate, is still not completely understood. Comparisons with phase diagrams of $C_{16}TAPA$ with $C_{16}TAB$ mixed with decanol showed that no inverted liquid crystalline phase are formed with the polymeric counterion, as opposed to the monomeric counterion bromide [12]. On the other hand, the complex salt with DNA, $C_{16}TADNA$, mixed with decanol and water also forms such an inverted phase, indicating an important contribution from features of the polyion [13].

Vesicles can be prepared by different techniques such as sonication, extrusion, surfactant removal, organic solvent evaporation or even spontaneously [1–4,14–18]. In this study, we focus on the sonication with a tip as the method used to prepare vesicles, which is one of the most suitable to prepare small vesicles [19].

Bordi and coworkers used DLS measurements to follow the time evolution of the aggregation behavior of mixtures of dioleoyltrimethylammonium propane (DOTAP)/sodium polyacrylate (NaPAA) and DOTAP–dipalmitoylphosphatidylcholine (DPPC)/NaPAA in aqueous solution. These mixtures gave rise to two kinds of structures with different sizes, whose time evolution depended on the ratio of charges and on the molar mass of the polyelectrolyte [20]. Clusters formed by polyion-coated vesicles, caused by interaction between DOTAP and NaPAA, were observed, with sizes that could be controlled by changes in the ionic strength [21].

Svensson et al. [22] proposed a new simplified approach to investigate mixtures of oppositely charged polymers and surfactants, involving the synthesis of complex salt of the ionic surfactants and polymers. Through this method, it was possible to investigate the phase behavior of truly binary mixtures of water and complex salts formed by cationic surfactants of different alkyl chain lengths ($n = 8$–16) with polyacrylate, and also ternary mixtures containing some of these complex salts and polyelectrolyte or cationic surfactants with different counterions [12,22–25].

Recently, Bernardes et al. [12,25] used this method to investigate the phase behavior of ternary mixtures containing alkyltrimethylammonium polyacrylate complex salt, water and different alcohols (used as co-surfactant or co-solvent). For mid- to long-chain alcohols, these systems displayed formation of a wide region of lamellar phases.

* Corresponding author.
E-mail address: wloh@iqm.unicamp.br (W. Loh).

This new approach differs from the conventional mixing of solutions of the oppositely charged polymer and surfactant, simplifying remarkably these studies and the interpretation of derived phase diagrams and related structural information [12,22–25]. Several studies have been reported on the interaction of polyions with vesicles [20,21,26–29], but the exact composition of vesicles is not known, only the global solution composition. Following this new approach, vesicles can be prepared from the pure complex salt and one can control exactly the composition of these vesicles, from neat polyion or mono-ion to their mixtures.

Despite the studies performed on mixtures between polyanions and cationic surfactants, one more detailed definition of the role of molecular parameters that govern the formation of these complex salts and their varied self-assembling structures is still incomplete.

In the present study, we performed an investigation on the effect of a polymeric counterion on the structure and thermotropic behavior of vesicles formed by complex salts DODAPA$_m$. These complex salts were based on the isolation of the complex salt formed by the mixtures of poly(acrylic acid) (PAA, containing 30 and 6000 units of acrylic acid) and the surfactant dioctadecyldimethylammonium bromide (DODAB). The properties of DODAPA$_m$ vesicles in aqueous solution was verified by high-sensitivity differential scanning calorimetry (HSDSC), dynamic light scattering (DLS), small-angle X-ray scattering (SAXS) and transmission electron microscopy (TEM). This study allowed the direct evaluation of the effect of polymeric counterion through comparison with properties of other vesicles formed with the monomeric counterions bromide and acetate.

2. Materials and methods

2.1. Materials

The cationic surfactant dioctadecyldimethylammonium bromide (DODAB) was purchased from Aldrich. Dioctadecyldimethylammonium acetate (DODAAc) was obtained by ion exchange from DODAB using a cationic ion-exchange resin, Dowex 550OH, from Sigma. The resin was activated by washing with 1 mol L^{-1} sodium acetate (NaAc) under stirring for 2 h, followed by thorough washing with Millipore water until neutral pH. Poly(acrylic acid), PAA, with molar masses of 2000 and 450,000 g mol^{-1} (ca. 30 and 6000 AA units, respectively), was obtained from Sigma. Both were used without further treatment. Water of Milli-Q quality was used throughout. n-decanol and n-tetradecanol from Fluka, with the highest purity available, were also used without further treatment.

2.2. Synthesis of complex salts

The complex salts DODAPA$_m$ (m = 30 and 6000) were prepared by mixing equimolar quantities of PAA$_m$ and DODAB under stirring. The PAA solution (50 mmol L^{-1}) was added dropwise to the DODAB dispersion (2 mmol L^{-1}) until the equimolar proportion. The precipitate formed was separated from the aqueous phase by filtration and rinsed with abundance of water. The complex salts were freeze-dried afterward. The product, a white hygroscopic powder, was stored in a desiccator over silica gel. Analysis of the bromide content of the supernatants, tested with aliquots of silver nitrate (AgNO$_3$) solution, confirmed that the ion exchange was complete, with no bromide detectable in the washing [12,13,25].

2.3. Preparation of vesicle dispersions

Films of DODAB, DODAAc, DODAPA$_{30}$ and their mixtures (1:1 mol) were prepared from chloroform solutions of the surfactants by evaporating the solvent under N$_2$ flux. After solvent evaporation,

the films remained over vacuum for 4 h at room temperature to ensure complete removal of the residual organic solvent. Vesicles were prepared by hydrating the films with 10–15 mL of aqueous solutions at 70 °C, followed by vortexing dispersions until they became homogeneously dispersed. Films of DODAPA$_{6000}$ and DODAPA$_{6000}$/DODAB (1:1 mol) mixtures were prepared from chloroform:methanol (1:1 volume) solutions of the surfactants by evaporating the solvent under N$_2$ flux. After organic solvent evaporation, the film was dispersed in chloroform:ethanol (3:1 volume) solution. The mixture was injected rapidly under vigorous stirring into an aqueous solution at 70 °C. The organic solvent removal was confirmed by additional stirring at 60 °C for 30 min. Stock solutions of vesicles were sonicated for 20 min (using an ultrasound tip) at 70 °C, approximately. After sonication, the dispersions were centrifuged for 1 h at 2000 rpm to remove dust/metal particles and multilamellae fragments that could be formed. The samples were then filtered through a 0.45-μm pore size filter to remove dust particles for the scattering studies. Vesicles dispersions at the desired concentration were obtained by direct dilution of the stock solutions. Solutions of vesicles with C$_{10}$OH or C$_{14}$OH in water were prepared from the stock solutions cited before and followed the same procedure. The dispersions of vesicles with C$_{10}$OH or C$_{14}$OH (1:1 by weight) in water were also sonicated for 20 min after addition of alcohols. The measurements were performed 24 h after vesicle preparation and repeated at least three times to check reproducibility. It is worth mentioning that the concentrations of the DODAPA$_{30}$ and DODAPA$_{6000}$ dispersions may not exactly be 0.4, 1, 10, 30 and 50 mmol L^{-1}, because it was not possible ensure their complete dispersion.

2.4. Dynamic light scattering (DLS) measurements

DLS studies were carried out using a Malvern Nano Zetasizer equipment with a 633-nm laser at 173°. All samples were analyzed at 25 °C. The Z-average diameter of the particles was obtained using the Stokes–Einstein equation. The polydispersity index (PDI) was calculated from the correlogram using the cumulants analysis. Repeatability of these results was confirmed by comparison among, at least, triplicates. The zeta potential of the vesicles was also analyzed and calculated applying Henry's equation.

2.5. High-sensitivity differential scanning calorimetry (HSDSC) measurements

A VP-DSC (MicroCal, Northampton, MA) calorimeter equipped with 0.542 mL twin cells for the reference and sample solutions was used. The measurements were performed with the scan rate of 1 °C min^{-1} and temperature range of 5–80 °C. The two cells filled with water were run as baseline for reference. From the thermograms, we obtained T_m as the temperature at the peak maximum.

2.6. Small-angle X-ray scattering (SAXS) measurements

The SAXS experiments were carried out using the SAXS beamline at the Brazilian Synchrotron Light Laboratory (LNLS) in Campinas, Brazil. The experimental setup involved the use of X-rays at the wavelength of 1.608 Å and a sample-to-detector distance of 611.1 mm. For these experiments, a sample cell with mica windows was used, allowing temperature control (measurements were made at 10, 25, 50 and 65 °C, with an accuracy better than 0.1°). The collected data were treated using the software FIT2D, which allows corrections for detector homogeneity, incident beam intensity, sample absorption and blank subtraction (the empty cell was considered as a blank). Typical acquisition times were ca. 5 min.

2.7. Transmission electron microscopy (TEM) measurements

TEM images were acquired using a Carl Zeiss CEM 902 transmission electron microscope at an accelerating voltage of 80 kV. Samples for TEM were prepared by the negative-staining technique with uranyl acetate solution (2%) as the staining agent. One drop of the solution was placed onto a carbon cooper grid. Filter paper was employed to remove the excess of sample. After 24 h, one drop of the uranyl acetate solution was placed onto the cooper grid, and the excess of liquid was also removed by filter paper.

3. Results and discussion

3.1. DLS results

Fig. 1 and Table 1 show the Z-average diameter and the zeta potential of DODAB, DODAAc and DODAPA$_m$ sonicated vesicles and for the mixtures DODAAc/DODAB, DODAAc/DODAPA$_{30}$ and DODAPA$_m$/DODAB (1:1 mol) in water as a function of time. The stability of these vesicles was examined by measuring vesicle Z-average diameter as a function of storage time at room temperature, that is, below their phase transition temperature (see Fig. 4). The dispersions were investigated at 1 mmol L^{-1} total surfactant concentration. It is worth reminding that for DODAPA$_{30}$ and DODAPA$_{6000}$, the concentration may not be exactly this. The Z-average diameters of sonicated vesicles lie in the range of 60–110 nm (Fig. 1 and Table 1), and the polydispersity indexes (PDIs) remained practically constant. The zeta potential values for DODAAc, DODAAc/DODAB and DODAAc/DODAPA$_{30}$ decrease with time, although the size of these vesicles remains roughly constant suggesting that, under these conditions, DODAAc induces the destabilization of vesicles. On the other hand, it is possible to observe an increase of zeta potential with time for DODAPA$_{6000}$ vesicles, from around 7–46 mV, with stable diameters (Fig. 1 and Table 1). These results are highly

Table 1
Values of Z-average size (D), zeta potential (ZP) and polydispersity index (PDI) of the sonicated vesicles without alcohol.

	D (nm)	ZP (mV)	PDI
DODAB	74	56 ± 2	0.24
DODAAc	66	52 ± 9	0.23
DODAPA$_{30}$	96	63 ± 4	0.22
DODAPA$_{6000}$	82	29 ± 6	0.23
DODAAc/DODAB	76	57 ± 9	0.25
DODAPA$_{30}$/DODAB	97	69 ± 5	0.23
DODAPA$_{6000}$/DODAB	85	65 ± 2	0.23
DODAAc/DODAPA$_{30}$	99	70 ± 10	0.25

reproducible as can be attested by the agreement observed for replicates, within a few %, among the average numerical values listed in Table 1.

The effect of C$_{10}$OH and C$_{14}$OH on the Z-average size and zeta potential of the sonicated vesicles (1:1 by weight) is shown in Fig. 2 and Table 2. Accordingly, a similar result is obtained by the dispersions without alcohol, showing diameters from 53 up to 104 nm. The size and PDI are maintained constant for at least 32 days, but DODAAc/C$_{10}$OH after 17 days exhibits a high polydispersity and reduction of zeta potential (Fig. 2 and Table 2). DODAB and DODAPA$_{30}$ with C$_{14}$OH also show a decrease in the zeta potential. The low zeta potential values show that there is no more indication of stability of these vesicles, inducing their flocculation. According to these zeta potential results, C$_{10}$OH causes more instability than C$_{14}$OH, as shown for low zeta potential values of DODAB, DODAAc and DODAPA$_{30}$. In general, the addition of C$_{14}$OH to the vesicle dispersions yields more stable vesicles than C$_{10}$OH. Additionally, the presence of C$_{14}$OH increases the size of vesicles.

3.2. HSDSC results

Fig. 1 of the supplementary material shows the HSDSC thermograms obtained for sonicated DODAPA$_{30}$ vesicles at selected
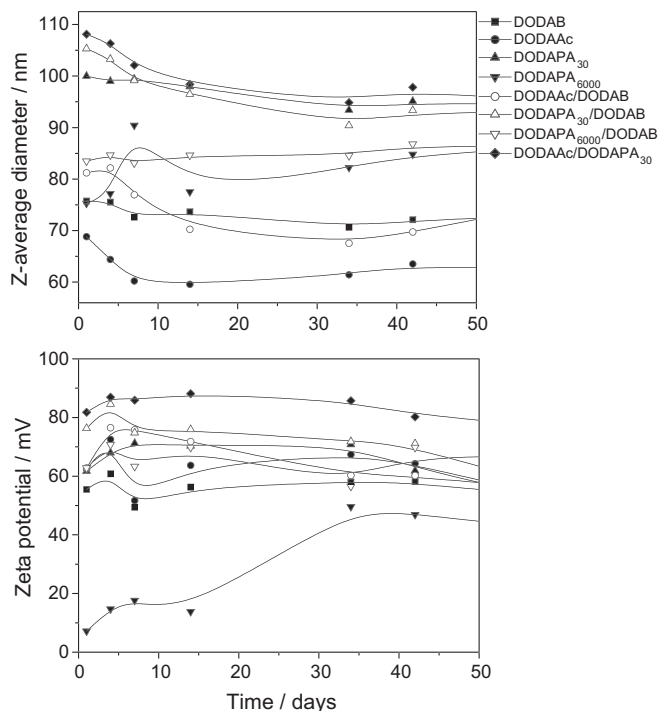
Fig. 1. Z-average diameter (a) and zeta potential (b) of sonicated DODAB, DODAAc, DODAPA$_m$ and mixed (1:1 in mol) DODAAc–DODAB, DODAAc/DODAPA$_{30}$ and DODAPA$_m$/DODAB dispersions as a function of time at 25 °C, for 1 mmol L^{-1} total surfactant concentration.
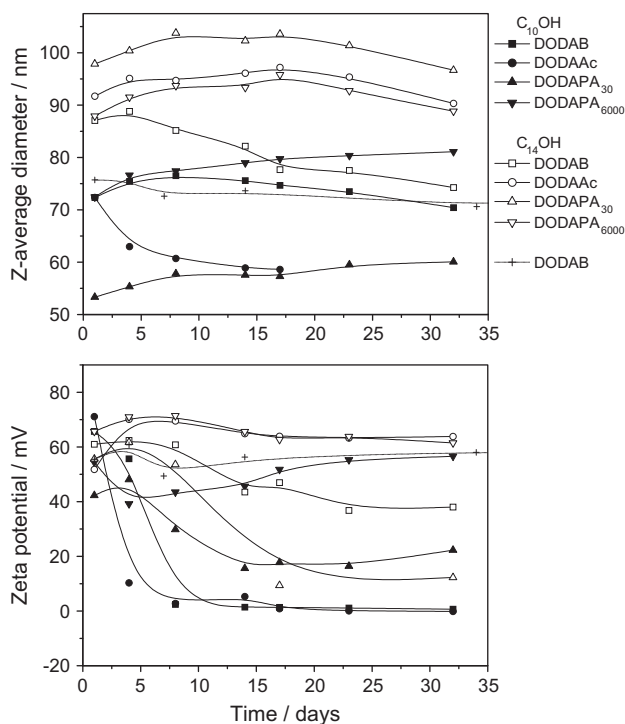
Fig. 2. Z-average diameter and zeta potential of sonicated DODAB, DODAAc, DODAPA$_m$ dispersions with C$_{10}$OH and C$_{14}$OH (1:1 by weigh) as a function of time at 25 °C.

Table 2
Values of Z-average size (D), zeta potential (ZP) and polydispersity index (PDI) of the sonicated vesicles with alcohol. (1:1 by weight).

	D (nm)	ZP (mV)	PDI
DODAB/C_{10}OH	74	18 ± 11	0.25
DODAAc/C_{10}OH	63	13 ± 10	0.43
DODAPA$_{30}$/C_{10}OH	57	28 ± 5	0.23
DODAPA$_{6000}$/C_{10}OH	78	50 ± 3	0.21
DODAB/C_{14}OH	82	50 ± 4	0.31
DODAAc/C_{14}OH	94	64 ± 2	0.26
DODAPA$_{30}$/C_{14}OH	101	47 ± 10	0.20
DODAPA$_{6000}$/C_{14}OH	92	66 ± 2	0.21

concentrations. The traces are shown in the same scale to allow a better visualization that the intensity increases with DODAPA$_{30}$ concentration. However, up to DODAPA$_{30}$ 10 mmol L^{-1}, surfactant concentration displays a minor effect on the transition temperatures. According to Feitosa et al. (2000), HSDSC results for DODAB non-sonicated vesicles exhibit T_m values roughly independent of concentration, but for sonicated dispersions, they decrease monotonically to the value characteristic of non-sonicated dispersions at about 1.0 up to 10 mmol L^{-1} [30]. In this work, we have chosen 10 mmol L^{-1} total surfactant concentration for HSDSC experiments for more evident curves.

HSDSC thermograms for sonicated DODAB, DODAAc and DODAPA$_m$ vesicles and the mixtures of DODAAc and DODAPA$_m$ with DODAB and DODAAc with DODAPA$_{30}$ in water at 10 mmol L^{-1} total surfactant concentration are shown in Fig. 3. Besides the gel to liquid crystalline transition temperature (T_m), neat DODAB vesicles exhibit a post-transition temperature (T_p), as reported before [17,31,32]. Under the same experimental condition, DODAPA$_{6000}$ and DODAPA$_{6000}$/DODAB vesicles exhibit a pre- and a post-transition in addition to the main transition. The pre-transition temperature (T_s) is related to the transition from the gel phase to the rippled gel phase, while the main transition is associated with the liquid crystalline phase, upon increasing temperature [33]. T_p is proposed to be related to changes in the local structure of the vesicular bilayer [32].

The nature of the surfactant counterion is of great importance on the phase behavior of ionic vesicles in general and cationic vesicles in particular. In the absence of inorganic salts, like NaBr or NaCl, T_m is higher for DODAC vesicles than for DODAB [30,34], probably due to specific affinity of counterions at vesicles interface. Moreover, NaCl increases, while NaBr decreases DODAB T_m in aqueous dispersions of vesicles prepared spontaneously, that is, in the presence of NaCl, DODAB vesicles resemble those of DODAC [34].

The effect of counterion nature on T_m of cationic vesicles was also investigated by Nascimento et al. [35]. Bromide, the least hydrated counterion studied, generates the lowest electrostatic repulsion between adjacent polar heads group, causing a less tightly packed hydrocarbon region than the chloride or acetate counterions.

The calorimetric scanning data for sonicated DODAB, DODAAc, DODAPA$_m$ and mixed DODAAc/DODAB, DODAPA$_{30}$/DODAAc and DODAPA$_m$/DODAB vesicles displayed in Fig. 3 shows that the neat DODAB dispersion exhibits two endothermic transitions at the temperatures T_m = 43.8 °C and T_p = 51.7 °C, in good agreement with values reported in previous publications [31,32]. Note that DODAPA$_{6000}$ and DODAPA$_{6000}$/DODAB presented similarly defined T_s and T_p peaks, besides that ascribed to T_m (Fig. 3). Here, it was not possible to observe a well-defined peak related to T_s for DODAB vesicles nor DODAPA$_{6000}$ and its mixture with DODAB. According to Fig. 3, a broader peak was also observed below that of the main transition for DODAB vesicles and this one was present for DODAAc, DODAPA$_m$ and in the mixed vesicles. This peak below T_m can be associated with the pre-transition temperature.

For all HSDSC curves, broader transitions were observed. The increase in peak width is attributed to decrease in cooperativity of the transition. Besides, it is known that peak broadening is typical of sonicated DODAB vesicles [36]. The broadening of these peaks is related to sharp transitions that may occur in a narrow range of temperature attributed to the different vesicle populations or bilayer structures formed in the dispersion, due to effect of sonication, for instance, such as small unilamellar vesicles, bilayer fragments or lens-like structures [30,37]. According to SAXS results (see Fig. 4), we observed the presence of multilayer vesicles (MLVs), probably favored by weaker intervesicular electrostatic repulsion between bilayers observed mainly in DODAPA$_m$ vesicle dispersions.

The counterions PA$_{30}^-$ and Ac$^-$ yield an increase of the stability of the DODAPA$_{30}$ and DODAAc vesicles in the gel phase associated with the observed increase in T_m relative to DODAB, while PA$_{6000}^-$ does not seem to affect T_m values of DODAPA$_{6000}$ and DODAPA$_{6000}$/DODAB vesicles, which showed similar melting temperatures. The presence of DODAB contributed to decreasing T_m values for mixed vesicles (Fig. 3), as expected, due to smaller value of T_m observed for this surfactant. The increase of T_m observed for DODAAc (47.3 °C) and DODAPA$_{30}$ vesicles (46.8 °C) compared to DODAB (43.8 °C) and DODAPA$_{6000}$ (44.2 °C) can be attributed to different affinity and binding specificity of the counterions to the vesicle interfaces. One should observe that the mixture DODAPA$_{30}$/DODAAc presented the melting temperature, T_m = 49.1 further higher than that shown for DODAAc and DOPAPA$_{30}$ vesicles. PA$_{30}^-$ and

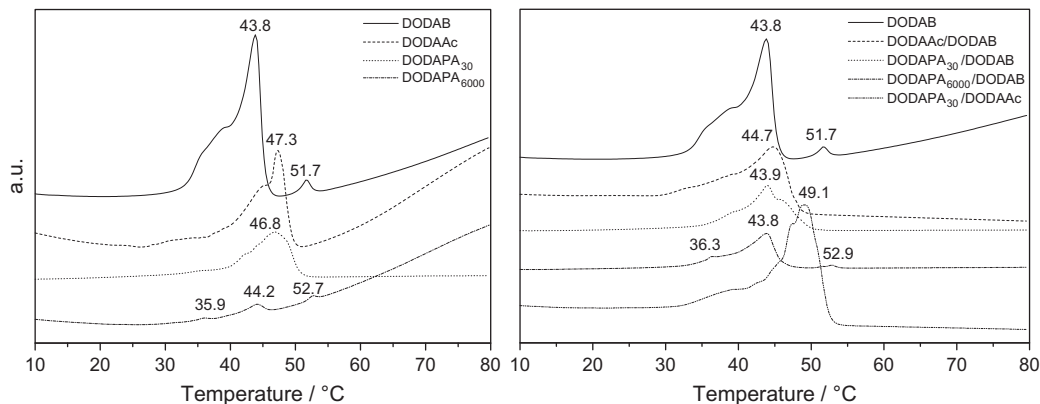**Fig. 3.** HSDSC upscan thermograms for sonicated DODAB, DODAPA$_m$ and DODAAc/DODAB, DODAPA$_{30}$/DODAAc and DODAPA$_m$/DODAB vesicles at 10 mmol L^{-1} total surfactant concentration.
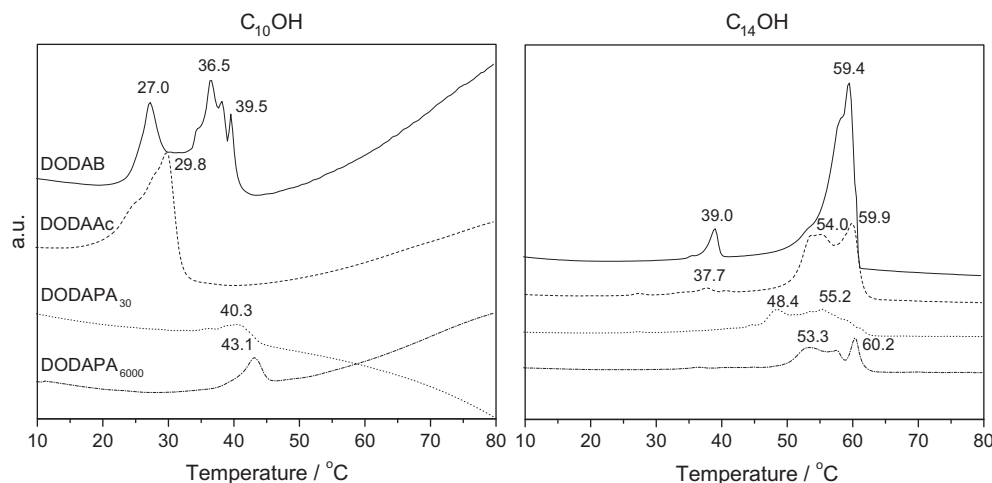
Fig. 4. HSDSC upscan thermograms for sonicated DODAB, DODAAc and DODAPA$_m$ vesicles mixed with C$_{10}$OH and C$_{14}$OH 4:1 (in mol) in aqueous solutions. The smaller Figure on the other side shows the expanded thermogram for DODAPA$_{30}$ and DODAPA$_{6000}$.

Ac$^-$ thus exhibit stronger effect turning the bilayers more rigid, yielding higher T_m values. The data shown above may be explained according to the degree of counterion association for the different counterions investigated in this work. The less hydrated counterion binds more strongly to the vesicle interface yielding smaller T_m values; thus, the binding strength follows the order Br$^-$ > PA$^-_{6000}$ > PA$^-_{30}$ > Ac$^-$.

The HSDSC upscan thermograms for sonicated DODAB, DODAAc and DODAPA$_m$ vesicles mixed with C$_{10}$OH and C$_{14}$OH (4:1 in mol) in aqueous solution are also shown in Fig. 4. In general, the presence of C$_{10}$OH decreases T_m of vesicle dispersions, except for DODAPA$_{6000}$, yielding a decrease of the thermal stability in the gel phase. There is a decrease of melting temperature observed for DODAAc and DODAPA$_{30}$ vesicles with C$_{10}$OH, T_m = 29.8 and 40.3 °C, respectively. For DODAPA$_{6000}$, the main transition remains roughly constant, T_m = 43.1 °C. The HSDSC profile of DODAB/C$_{10}$OH is different than for the vesicles with counterions Ac$^-$, PA$^-_{30}$ and PA$^-_{6000}$. The main transition peak of DODAB/C$_{10}$OH divides into three endothermic transitions at the temperatures T_{m1} = 36.5, T_{m2} = 38.3 and T_{m3} = 39.5 °C that may be attributed to the different bilayer structures in the dispersion. Other defined peak centered at 27.1 °C is also observed (compare Fig. 3 with Fig. 4). The presence of C$_{10}$OH inside the bilayer vesicles causes an overall disordering effect on the hydrocarbon chains packing, thus decreasing T_m. As observed in Fig. 3, a broader peak below main transition, which was associated with the T_s for the vesicles without C$_{10}$OH, is also observed below T_m of DODAB, DODAAc and DODAPA$_{30}$, but DODAPA$_{6000}$ does not show any pre-transition peak.

For sonicated DODAB, DODAAc and DODAPA$_m$, vesicles mixed with C$_{14}$OH (4:1 in mol) in aqueous solution are also shown in Fig. 4. On the contrary as observed for dispersions containing C$_{10}$OH, the presence of C$_{14}$OH increases T_m of vesicle dispersions. In this case, the thermograms of DODAAc, DODAPA$_{30}$ and DODAPA$_{6000}$ vesicles present the same behavior, which is three main transitions observed in a single peak, starting at about 48 up to 60 °C, while DODAB shows a single endothermic transition at T_m = 59.4 °C. Through Fig. 4, it is possible also to observe one shoulder below T_m of DODAB. For the vesicles containing the counterions Ac$^-$, PA$^-_{30}$ and PA$^-_{6000}$, this shoulder is divided in two endothermic peaks, showing practically the same behavior that may be related to the different distribution of C$_{14}$OH inside vesicle bilayers. Besides, T_s appears in all thermograms curves in the presence of C$_{14}$OH. The well-defined peak observed for DODAB/C$_{10}$OH at 27.1 °C is also shown for DODAPA$_{6000}$/C$_{14}$OH at 27.1 °C in the expanded thermogram at Fig. 4.

The DSC curves (Fig. 4) indicate that the longer the alcohol chain length, the more intense the pre-transition peak, being more defined for DODAB and DODAAc dispersions. Tetradecanol, however, shows more defined T_s in the vesicles than decanol or than sonicated vesicles without alcohol. Moreover, the incorporation of C$_{14}$OH into the vesicle bilayer yields a more organized bilayer, thus increasing all of the transition peaks.

3.3. SAXS results

Vesicle dispersions of sonicated DODAB, DODAAc, DODAPA$_m$ and the mixtures DODAPA$_m$/DODAB and DODAPA$_{30}$/DODAAc up to 50 mmol L^{-1} total concentration in water were investigated by small-angle X-ray scattering (SAXS) measurements at 25 and 50 °C. Results are shown in Fig. 5 and Table 3. SAXS measurements are capable of providing information about the bilayer structure and vesicle morphology. The bilayer repeat distance or lamellar thickness d in the vesicles was obtained through the Bragg peak relation $d = (2\pi/q)$, with q, the wave vector, corresponding to the maximum intensity of the Bragg reflection.

SAXS scattering data for DODAAc at 25 and 50 °C and the mixture DODAAc/DODAB at 25 °C do not present any Bragg peaks at concentrations up to 50 mmol L^{-1}, but DODAAc/DODAB dispersions exhibit a peak around d = 2.0 nm at 50 °C (Fig. 2 of the supplementary material). The absence of peak may be explained by the formation of mostly unilamellar vesicles. The Bragg peaks for DODAB 30 mmol L^{-1}, DODAPA$_{30}$ and DODAPA$_{30}$/DODAB 10 mmol L^{-1}, are always located at q = 1.7 nm at 25 °C, corresponding to repeat distances around 3.6 nm evidencing formation of MLV dispersed in water. This value is in good agreement with that reported for the neat DODAB lamellae, dispersed in water at 30 °C [38]. The same value is observed for DODAPA$_{30}$/DODAAc dispersions at 10 mmol L^{-1} at 50 °C, maintaining similar behavior with increasing temperature. DODAPA$_{6000}$ and DODAPA$_{6000}$/DODAB 30 and 50 mmol L^{-1} show the same d = 3.6 nm at 25 °C. A narrow peak with much higher intensity, followed by others that can be ascribed to higher order reflections, was observed for DODAPA$_{6000}$ 50 mmol L^{-1} at 25 °C, a characteristic behavior indicating the formation of lamellar structures (see Fig. 3 of the supplementary material) [39].

Sonication is a method of vesicle preparation expected to produce mostly unilamellar vesicles at low surfactant concentrations. In the present investigation, for samples prepared at low concentrations, below 1 mmol L^{-1}, as observed by TEM pictures in Fig. 7, it was difficult to distinguish whether uni- or multilamellar
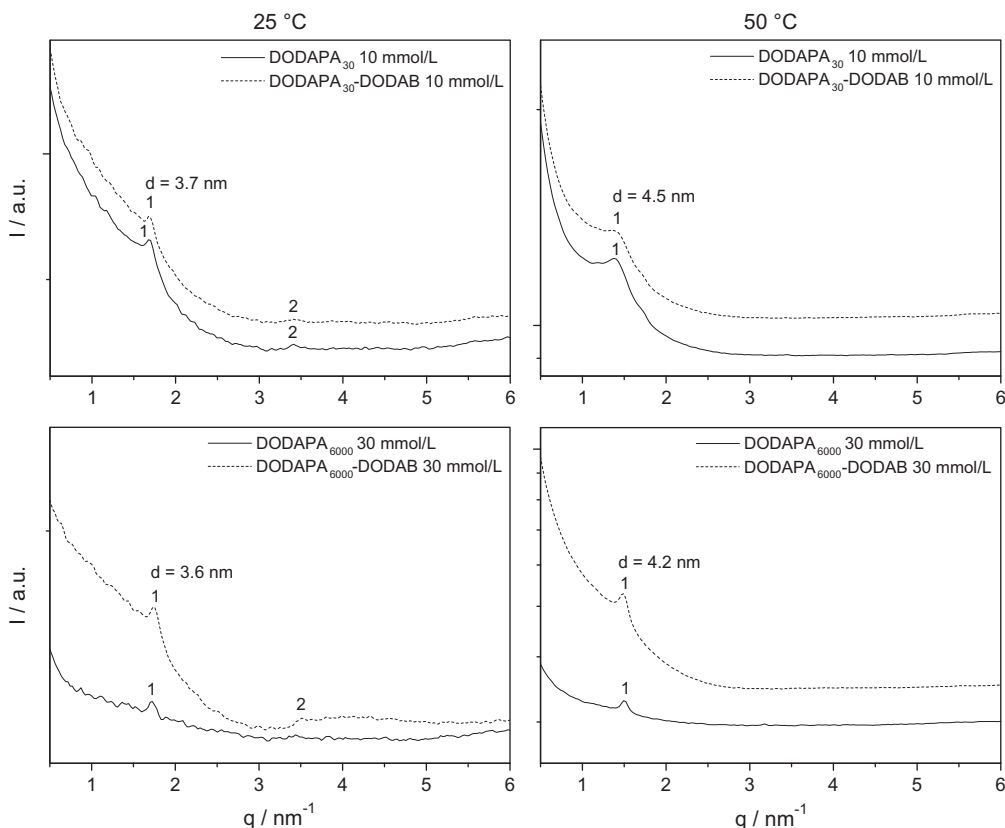
Fig. 5. SAXS curves for sonicated DODAB, DODAAc, DODAPA$_m$ and the mixtures DODAPA$_m$/DODAB and DODAPA$_{30}$/DODAAc dispersions in water at 25 and 50 °C.

vesicles were obtained. For the samples prepared for SAXS analyses, which required greater concentrations (above 10 mmol L^{-1}) to allow for scattering detection, multiple peaks were observed, ascribed to reflections of a lamellar geometry consistent with the formation of multilamellar vesicles, as pointed out by earlier literature reports [40,41]. Unfortunately, none of the techniques (SAXS or TEM) could be applied to samples at the same concentration; hence, we can only propose that polyions favor the assembling of bilayers associated with MLV formation, in a similar way to what has been observed with lamellar phases of these complex salts [12,25,42]. The larger values of d observed at 50 °C, i.e., 4.3 ± 0.3 nm for DODAPA$_{30}$ and DODAPA$_{30}$/DODAB 10 mmol L^{-1}, 4.0 ± 0.3 nm for DODAPA$_{6000}$ and DODAPA$_{6000}$/DODAB in both concentrations (30 and 50 mmol L^{-1}), may be ascribed to an increase of dissociation degree and/or bilayer repulsion, leading to an increase of water layer thickness (d_w). Typically above T_m, in the liquid crystalline phase, a decrease in the repeat distance is expected, considering that d is the lamellar thickness plus d_w between bilayers in MLV. Mertins et al. [43] also suggested an increase of d_w due to larger d with increasing temperature for phosphatidylcholine (PC) and PC/chitosan vesicles. Through Fig. 3 of the supplementary material, it is possible to observe a transition from lamellar phase to MLV dispersion for DODAPA$_{6000}$ at 50 mmol L^{-1} with increasing temperature, which can be related to an increase of bilayer flexibility at higher temperatures.

Studies of mixtures of other cationic surfactants with polymeric counterions forming lamellar phases mixed with C$_{10}$OH presented d values varying from 3.8 to 4.8 nm [12,25], which are close to values determined in the present investigation. This behavior may be attributed to different values of d_w, in spite of difference in the surfactant chain length, that is, number of carbon in the chain hydrocarbon varying from C$_{12}$ to C$_{18}$.

Preliminary studies using SASfit software to fit our SAXS data to surfactant bilayers revealed that is possible to obtain a good fitting for the spectrum obtained using sonicated DODAB vesicles with C$_{10}$OH at 10 °C (Fig. 4 of the supplementary material). Through this analysis, the thickness of the inner part of the surfactant bilayer can be estimated as t_h = 2.90 nm. This value can be compared to d_{hc} values reported for lamellar phases formed by C$_{16}$TAPA$_{30}$ and C$_{16}$TAPA$_{6000}$ with water and decanol, which were found to vary between 2.1 and 3.0 nm [12,25], considering that larger values are expected because of the longer dioctadecyl chain. Assuming the bilayer thickness as constant and equal to 3.0 nm, the thicknesses of the water layers, d_w, in sonicated vesicles were estimated and are listed in Tables 3 and 4.

Vesicle dispersions of sonicated DODAB, DODAAc and DODAPA$_m$ mixed with C$_{10}$OH and C$_{14}$OH (4:1 in mol) in aqueous solutions were also investigated by small-angle X-ray scattering (SAXS) measurements at 10, 25, 50 and 65 °C. All dispersions with C$_{10}$OH were measured at 10, 25 and 50 °C, while dispersions with C$_{14}$OH were prepared at 25, 50 and 65 °C (Fig. 6). These temperatures were chosen due to lower and higher T_m values presented by HSDSC results, respectively. In general, all of these curves present the same behavior, showing broader peaks with low intensity. According to these results, the presence of both alcohols inside the vesicle bilayer causes d values to decrease slightly with increasing temperature.

SAXS curves for DODAAc in the presence of C$_{10}$OH do not show any Bragg peaks at 25 and 50 °C (Fig. 5 of the supplementary material). The absence of peak can also be associated with the formation of unilamellar vesicles, as described previously for vesicles without alcohol. The Bragg peaks for DODAB, DODAPA$_{30}$ and DODAPA$_{6000}$ at 25 °C are associated with d values of 4.5, 5.2 and 5.7 nm, respectively, indicating again formation of MLV in water (Fig. 6 and Table 3). The smaller values of d = 3.1, 4.5 and 3.7 nm observed for DODAB,
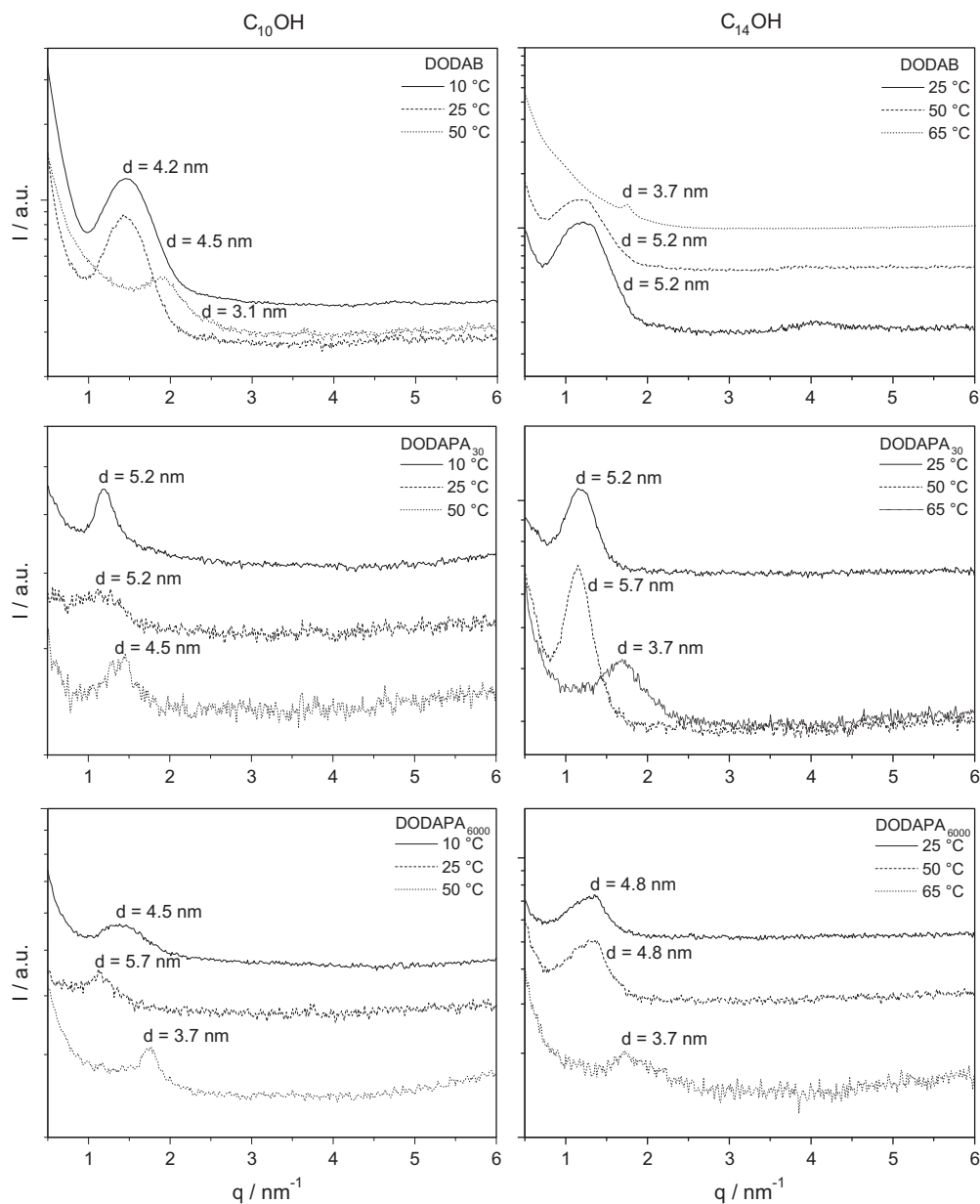
Fig. 6. SAXS curves of sonicated DODAB, DODAAc and DODAPA$_m$ mixed with C$_{10}$OH and C$_{14}$OH (4:1 in mol) dispersions in aqueous solution at 10, 25, 50 and 65 °C.
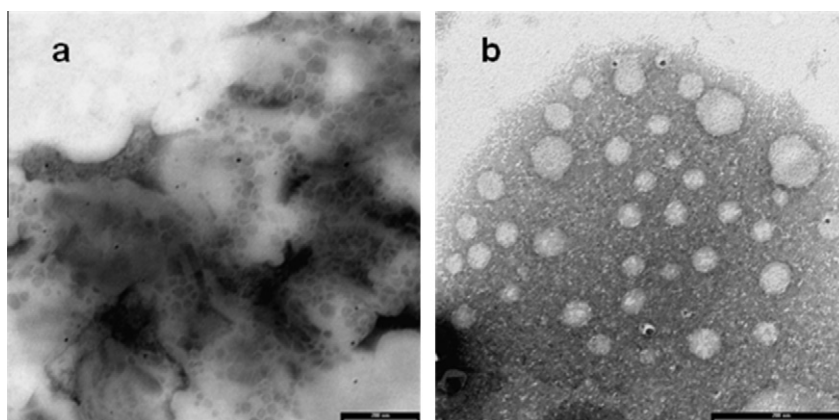

Fig. 7. TEM images (negative staining) of sonicated vesicles formed by DODAPA$_{30}$ (a) and DODAPA$_{6000}$ (b) 400 μmol/L in aqueous dispersion. Bar is 200 nm.

Table 3
Values of repeat distance (d) of the sonicated vesicles without alcohol at 25 and 50 °C.
d_{hc} = 3.0 nm.

	$d_{25 °C}$ (nm)	$d_{50 °C}$ (nm)	$d_{w25 °C}$ (nm)	$d_{w50 °C}$ (nm)
DODAB	3.6 ± 0.1	3.7	0.6	0.7
DODAAc	4.2	–	1.2	–
DODAPA$_{30}$	3.7	4.4 ± 0.1	0.7	1.4
DODAPA$_{6000}$	3.6	3.9 ± 0.2	0.6	0.9
DODAAc/DODAB	3.6	–	0.6	–
DODAPA$_{30}$/DODAB	3.7	4.2 ± 0.3	0.7	1.2
DODAPA$_{6000}$/DODAB	3.6	4.0 ± 0.2	0.6	1.0

Table 4
Values of repeat distance (d) of the sonicated vesicles with alcohol at 25, 50 and 60 °C.
(1:1 by weight). d_{hc} = 3.0 nm.

	$d_{25 °C}$ (nm)	$d_{50 °C}$ (nm)	$d_{60 °C}$ (nm)	$d_{w25 °C}$ (nm)	$d_{w50 °C}$ (nm)	$d_{w60 °C}$ (nm)
DODAB/ C$_{10}$OH	4.5	3.1	–	1.5	0.1	–
DODAAc/ C$_{10}$OH	–	–	–	–	–	–
DODAPA$_{30}$/ C$_{10}$OH	5.2	4.5	–	2.2	1.5	–
DODAPA$_{6000}$/ C$_{10}$OH	5.5 ± 0.3	3.7	–	2.5 ± 0.3	0.7	–
DODAB/ C$_{14}$OH	5.2	5.0 ± 0.2	3.7	2.2	2.0 ± 0.2	0.7
DODAAc/ C$_{14}$OH	5.2	–	–	2.2	–	–
DODAPA$_{30}$/ C$_{14}$OH	5.2	5.7	3.8 ± 0.1	2.2	2.7	0.8 ± 0.1
DODAPA$_{6000}$/ C$_{14}$OH	4.8	3.7/4.5	3.7 ± 0.1	1.8	0.7/1.5	0.7 ± 0.1

DODAPA$_{30}$ and DODAPA$_{6000}$ at 50 °C, contrary to those observed in the absence of alcohol, cannot be attributed to dehydration of vesicle bilayers uniquely. These results can also be explained by the mismatch of the chain length between C$_{10}$OH and DODA$^+$, causing more disorder in the vesicle bilayer than without C$_{10}$OH. In this case, at 25 and 50 °C, these vesicles are in the gel and liquid crystalline states, respectively.

As for the data for vesicles with C$_{14}$OH, a similar behavior is observed (Fig. 6). The bilayer thickness also decreases with increasing temperature, from 25 (gel) to 65 °C (liquid crystalline). SAXS spectrum with DODAAc shows only a shoulder around d = 5.2 nm at 25 °C (Fig. 4 of the supplementary material). In Fig. 6, at 25 °C, the d values are 5.2 nm for DODAB and DODAPA$_{30}$ and 4.8 nm for DODAPA$_{6000}$. On the other hand, the SAXS spectra for DODAB, DODAPA$_{30}$ and DODAPA$_{6000}$ display the same d = 3.7 nm at 65 °C (liquid crystalline phase), independent of the counterions, suggesting effects from the latter are not so relevant.

Comparing SAXS data of the dispersions with and without alcohol, one observes that both alcohols decrease the vesicle repeat distances, what may be ascribed to the mismatch between the alcohols and surfactant alkyl chain length, rather than to their effect on bilayer ordering (which are opposite as indicated by their thermotropic behavior).

3.4. TEM results

DODAPA$_{30}$ and DODAPA$_{6000}$ vesicles at 0.4 mmol L^{-1}, prepared by sonication, were also examined by transmission electron microscopy (TEM). As observed in the TEM images, the vesicles prepared by DODAPA$_{30}$ and DODAPA$_{6000}$ (Fig. 7) display sizes and

polydispersity in agreement with the values determined by DLS, as expected for the sample prepared by sonication. The dominant structures in the micrograph were spherical vesicles. Few large spherical vesicles were observed for both vesicles, indicating fusion between vesicles. In order to use this methodology, rather dilute dispersions had to be prepared (in this case, much more dilute than the ones analyzed by SAXS, for instance). In this concentration, no sign of MLV formation was observed in the micrographs. However, because MLV formation is expected to be favored by increase in concentration, we cannot determine whether uni- or multilamellar vesicles will be present at the higher concentrations used in the SAXS and DLS analyses, but it is clear that their sizes, with diameters varying approximately from 70 to 120 nm, agree well with the values derived from DLS measurements, confirming that vesicles are formed and that they are the predominant structures obtained with these complex salts and the sonication methodology.

4. Conclusions

The present investigation reports on liposome preparation using polyelectrolyte–surfactant complex salts. To the best of our knowledge, this is the first report using these substances and their mixtures, therefore with direct control over the system composition (stoichiometry). Overall, these results confirm the possibility of preparing liposomes using this methodology in a simple and controlled way. In general, properties of these liposomes do not differ significantly from those previously reported for liposomes prepared by addition of polyelectrolytes over surfactant liposomes. Results from the present investigation did not detect significant difference in liposome properties (size, surface potential, thermotropic transitions and kinetic stability) for liposomes with monomeric or polymeric counterions, the latter probed with both short and long polyions. This finding may explain the agreement observed between the two methodologies. Once more, it is important to stress that this conclusion could only be unequivocally established through an investigation with exact control over the system composition (stoichiometry), such as the present one.

However, there was one important difference in the properties of liposomes containing monomeric and polymeric counterions observed in the present study, namely the polymer induced formation of multilamellar vesicles. SAXS analyses also confirmed that the thickness of the aqueous regions between surfactant bilayers was small enough to allow for bridging effects for both the short and long polyanions, which may explain the favoring of these multilamellar aggregates. These findings also agree with observations from earlier studies on lamellar systems formed by these complex salts, when compared to lamellae formed with monomeric counterions [12,42,22–24]. Although these multilamellar vesicles did not show differences in the studied properties with respect to unilamellar ones (obtained with monomeric counterions), they may offer interesting possibilities for other studies, for instance, related to active encapsulation or controlled release, for instance, in which the presence of multicompartments or barriers may be sought.

Appendix A. Supplementary material

Supplementary data associated with this article can be found, in the online version, at doi:10.1016/j.jcis.2011.11.020.

References

[1] J.H. Fendler, Membrane Mimetic Chemistry, Wiley-Interscience, New York, 1982.
[2] D.D. Lasic, Liposomes. From Physics to Applications, Elsevier, Amsterdam, 1993.
[3] G. Cevc (Ed.), Phospholipid Handbook, Marcel Dekker, New York, 1993.
[4] J.B.F.N. Engberts, D. Hoeskstra, Biochim. Biophys. Acta 1241 (1995) 323–340.
[5] C.W. Pouton, L.W. Seymour, Adv. Drug Deliver. Rev. 34 (1998) 3–19.
[6] D.D. Lasic, Liposomes in Gene Delivery, CRC Press, Boca Raton, FL, 1997.
[7] D.D. Lasic, N.S. Templeton, Adv. Drug Deliver. Rev. 20 (1996) 221–266.
[8] S. Liu, G. Lu, Biophys. Chem. 127 (2007) 19–27.
[9] P.C.A. Barreleiro, B. Lindman, J. Phys. Chem. B 107 (2003) 6208–6213.
[10] P.C.A. Barreleiro, R.P. May, B. Lindman, Faraday Discuss. 122 (2002) 191–201.
[11] P.C.A. Barreleiro, G. Olofsson, P. Alexandridis, J. Phys. Chem. B 104 (2000) 7795–7802.
[12] J.S. Bernardes, J. Norrman, L. Piculell, W. Loh, J. Phys. Chem. B 110 (2006) 23433–23442.
[13] A. Bilalov, C. Leal, B. Lindman, J. Phys. Chem. B 108 (2004) 15408–15414.
[14] A.M. Carmona-Ribeiro, Chem. Soc. Rev. 21 (1992) 209–214.
[15] E. Feitosa, J. Jansson, B. Lindman, Chem. Phys. Lipids 142 (2006) 128–132.
[16] I.M. Cuccovia, A. Sesso, E.B. Abuin, P.F. Okino, P.G. Tavares, J.F.S. Campos, F.H. Florenzano, H. Chaimovich, J. Mol. Liquids 72 (1997) 323–336.
[17] E. Feitosa, W. Brown, Langmuir 13 (1997) 4810–4816.
[18] P. Saveyn, J. Cocquyt, P. Bomans, P. Frederik, M. De Cuyper, P. Van der Meeren, Langmuir 23 (2007) 4775–4781.
[19] A.M. Carmona-Ribeiro, H. Chaimovich, Biochim. Biophys. Acta 733 (1983) 172–179.
[20] F. Bordi, C. Cametti, D. Gaudino, S. Sennato, Bioeletrochemistry 59 (2003) 99–106.
[21] F. Bordi, C. Cametti, S. Sennato, Chem. Phys. Lett. 409 (2005) 134–138.
[22] A. Svensson, L. Piculell, B. Cabane, P. Iiekti, J. Phys. Chem. B 106 (2002) 1013–1018.
[23] A. Svensson, L. Piculell, L. Karlsson, B. Cabane, B. Jönsson, J. Phys. Chem. B 107 (2003) 8119–8130.
[24] A. Svensson, J. Norrman, L. Piculell, J. Phys. Chem. B 110 (2006) 10332–10340.
[25] J.S. Bernardes, W. Loh, J. Colloid Interface Sci. 318 (2008) 411–420.
[26] A.A. Yaroslavova, O.Ye. Kuchenkovaa, I.B. Okunevaa, N.S. Melik-Nubarova, N.O. Kozlovaa, V.I. Lobyshevb, F.M. Mengerc, V.A. Kabanov, Biochim. Biophys. Acta 1611 (2003) 44–54.
[27] V.A. Kabanov, A.A. Yaroslavova, J. Controll. Release 78 (2002) 267–271.
[28] M.G. Miguel, A.A.C.C. Pais, R.S. Dias, C. Leal, M. Rosa, B. Lindiman, Colloids Surf. A 228 (2003) 43–55.
[29] F.E. Antunes, E.F. Marques, M.G. Miguel, B. Lindman, Adv. Colloid Interface Sci. 147 (2009) 18–35.
[30] E. Feitosa, P.C.A. Barreleiro, G. Olofsson, Chem. Phys. Lipids 105 (2000) 201–213.
[31] F.R. Alves, M.E.D. Zaniquelli, W. Loh, E.M.S. Castanheira, M.E.C.D. Real Oliveira, E. Feitosa, J. Colloid Interface Sci. 316 (2007) 132–139.
[32] F.R. Alves, E. Feitosa, Thermochim. Acta 472 (2008) 41–45.
[33] D.F. Evans, H. Wennerström, The Colloidal Domain: Where Physics, Chemistry, Biology and Technology Meet, second ed., Wiley/VCH, New York/Weinheim, 1999.
[34] E. Feitosa, P.C.A. Barreleiro, Progr. Colloid Polym. Sci. 128 (2004) 163–168.
[35] D.B. Nascimento, R. Rapuano, M.M. Lessa, A.M. Carmona-Ribeiro, Langmuir 14 (1998) 7387–7391.
[36] J. Cocquyt, U. Olsson, G. Olofsson, P. Van der Meeren, Langmuir 20 (2004) 3906–3912.
[37] R.O. Brito, E.F. Marques, Chem. Phys. Lipids 137 (2005) 18–28.
[38] M. Jung, A.L. German, H.R. Fischer, Colloid Polym. Sci. 279 (2001) 105–113.
[39] J.A. Bouwstra, G.S. Gooris, W. Bras, H. Talsma, Chem. Phys. Lipids 64 (1993) 83–98.
[40] O. Mertins, M.B. Cardoso, A.R. Pohmann, N.P. Silveira, J. Nanosci. Nanotechnol. 6 (2006) 2425–2431.
[41] N. Kucerka, Mu-P. Nieh, J. Katsaras, Advances in Planar Lipid Bilayers and Liposomes, vol. 12, Elsevier, 2010.
[42] J.S. Bernardes, L. Piculell, W. Loh, J. Phys. Chem. B 115 (2011) 9050–9058.
[43] O. Mertins, M.I.Z. Lionzo, Y.M.S. Micheletto, A.R. Pohlmann, N.P. Silveira, Mater. Sci. Eng. C 29 (2009) 463–469.